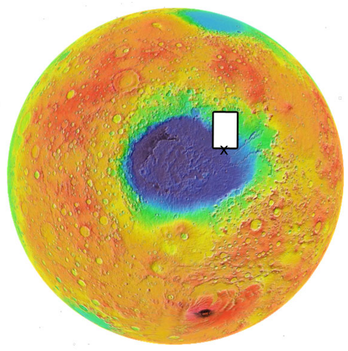
Mapping Channel Belt Fluvial Deposits on Mars

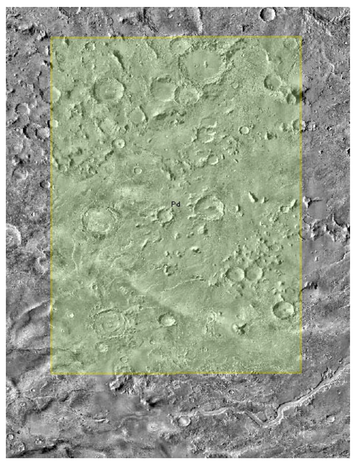
"CARTOGRAPHY BEYOND THE ORDINARY WORLD"
JOINT ICA SYMPOSIUM
Fluminense Federal University, 21–22 August, 2015

H. I. Hargitai[1], V. Gulick[2]

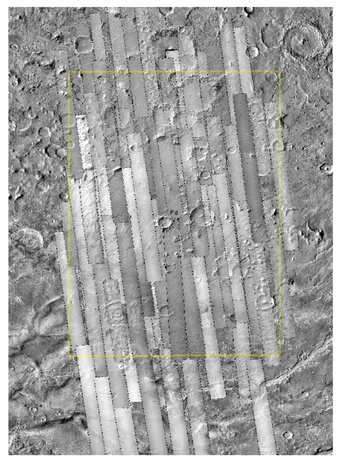
1 NASA Ames Research Center / NPP, MS 239-20, Moffett Field, CA 94035, USA, henrik.i.hargitai@nasa.gov
2 NASA Ames Research Center/ SETI Institute, MS 239-20, Moffett Field, CA 94035, USA



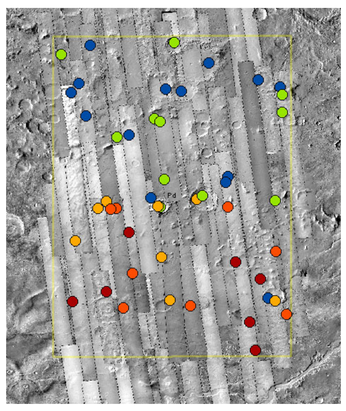
Research area is North-East of Hellas Basin. This area features unusually small outflow-like valleys and a wedge-shaped plain that is eroded into the basin rim. No geologic mapping has been done in this area. We have identified evidence for paleolake basins and channels in this area. The area is ca. 225.000 km².



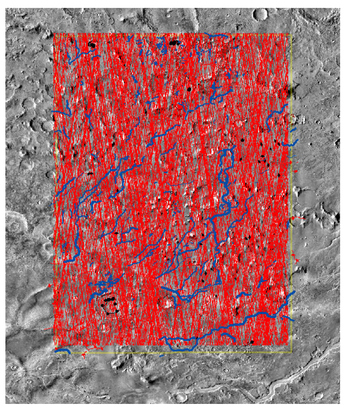
An ArcGIS geodatabase is made in equirectangular projection. A THEMIS Day IR global mosaic and a global MOLA DEM is added. The THEMIS image serves as basemap for georeferencing higher resolution CTX images. For better mapping and interpretation, we used the global THEMIS Night IR mosaic which shows surface material's thermal inertia that can be used to distinguish loose materials, e.g., sediments (dark) from bedrock (bright).



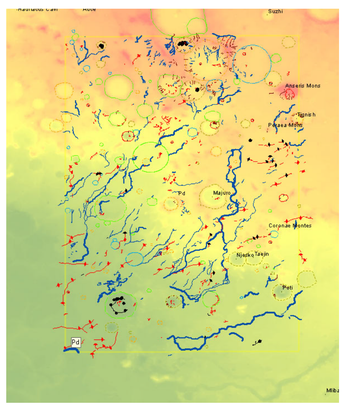
All available CTX images are added. Original labels of CTX images show different offsets, which made it necessary to manually georeference each CTX image. Where no CTX was available, we used HRSC ND4 images as fillers. The still remaining areas are mapped using lower resolution THEMIS Day IR.



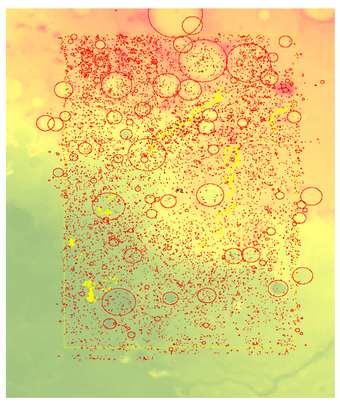
Sporadic HiRISE and CRISM data are color-coded and added as point data. This map shows how large area on a single HiRISE frame is covered by pitted smooth deposit, interpreted as degraded latitude dependent mantle. (blue 0% carmine 100%)



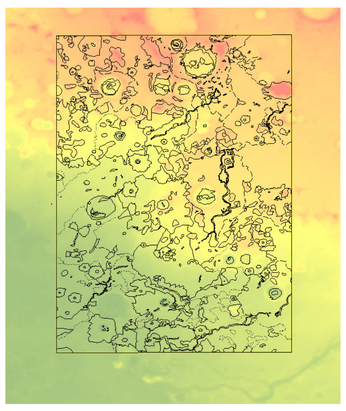
MOLA PEDR tracks are added for precise channel depth and channel long profile measurements. Most channels are too narrow to be visible on either on MOLA MEGDR (interpolated DEM) or stereo-derived HRSC DA4 DEMs.



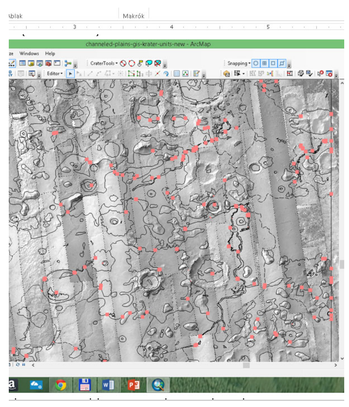
Channels and valleys and other structural features (wrinkle ridges, sinuous ridges, faults etc.) are mapped. In this map the line width of channels is proportional to real width. Channel reaches are also categorized according to depth and reach type (bedrock - erosional or alluvial - depositional). Crater rims are also outlined and categorized according to rim degradation.



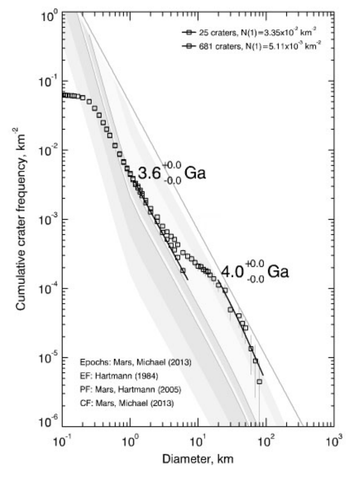
Crater counting was undertaken using CraterTools integrated into ArcGIS. Craters are counted in the whole mapping area to give the most accurate age data for each surface cover unit. Craters larger than 300 m in diameter are counted in the whole area, all craters visible in CTX (about 10 m) are counted in wide-channel floor deposits. In total, 15500 craters were counted. Secondary crater rows, fields and irregular craters are ignored.



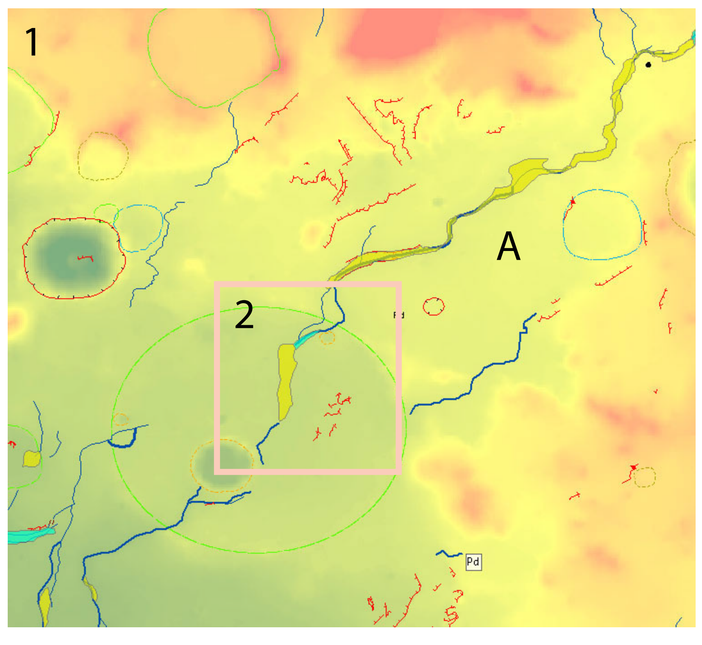
Photogeologic mapping: visible contacts are mapped to make a surface cover (?material unit?) map. Accurate contacts are drawn from CTX visible morphology, gradual or approximate contacts are those of some ejecta, or plains, and inferred contacts are those identified from THEMIS Night IR data. Although these are sharp boundaries on the night IR images, they do not necessarily appear on Day IR or CTX data. They, however appear on visible HRSC data as bright/dark unit boundaries. Wide-channel fills and smooth terminal and overbank deposits are also mapped as separate unit.



The line work topology errors must be fixed before polygons can be made. Polygons will serve as geologic units on the map. Neighboring polygon boundaries must precisely overlap. Topology rules help find line intersections, overlaps, and dangles. All errors are corrected manually and validated. Delineated features are converted to polygons.



Noncontiguous units are integrated and their age is determined using CraterStats software. For large, continuous units, different counting areas are tested to determine smallest accurately measurable unit size. In this diagram, all craters from the whole area are shown, showing that the overall surface is 4.0 Ga old and a resurfacing - possibly lava emplacement - event occurred at 3.6 Ga, and the surface was eroded since.
Crater dating of units and stratigraphic relations together will determine the sequence of unit formations (i.e. the inferred evolution in the research area). This will be shown in the form of COMU (correllation of map units) on the map.



Thematic mapping reveals the sequential nature of channels in the area, which probably depends on local topography and lithology. Reaches where the channel is cut into the bedrock are alternating with reaches where the channel is filled in by - nonterminal - sediments. In these reaches the channel walls disappear. The channel, however, reappears downstream. We interpret this as an area of possible infiltration into the subsurface and subsequent outflow to surface.
Figure C shows a system where the channel heads are cut into Pb onto which another upstream channel deposited its sediments.

Introduction: Fluvial deposits are a key geological unit in the search for water and sites where ancient life could have been supported. Recently an increasing number of features are identified as fluvial sedimentary units [1-9]. For example deposits on the lee sides of intrachannel obstacles, typically craters, , antidunes or transverse ribs [3,4], and flood-formed dunes [1,2]. However, some of these interpretations are challenged by volcanic models [10-12].

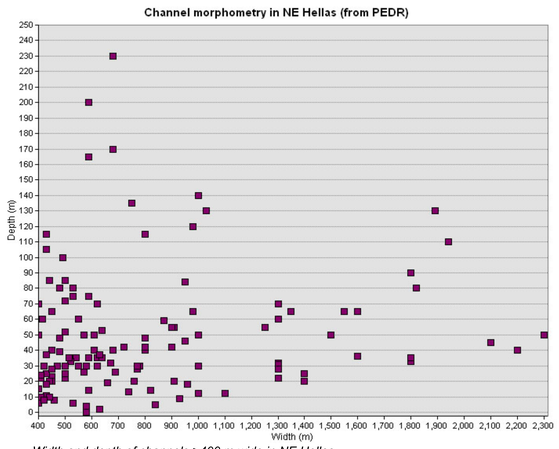
Methods. We mapped two, approx. 500 km long channel and valley systems on the plains NE of Hellas Basin. The systems consist of wide, outflow-like channel reaches and narrow valleys and sections with positive elevation, proposed to be fluvial deposits. The major objective of this study is to find evidence of fluvial deposits associated with channels on Mars.

We used ArcMap 10.1 software. For general mapping and feature identification, we used a mosaic of MRO CTX images, with THEMIS Day IR, HRSC ND4 and IHS images as fillers. For material unit identification, we used THEMIS Night IR, HRSC color, CRISM and HiRISE images. We used the MOLA PEDR dataset to determine channel depths >400 m wide (PEDR data points have a spacing of 300 m so for narrower channels there was no channel-crossing track point in the middle of the channel). The longitudinal channel profiles are approximately linear (neither concave or convex) measured from the source to the end of the channel systems. Although narrow channels are typically shallower than wide channels, the deepest channels are also narrow, suggesting that those narrow channels erode vertically while wide channels typically erode laterally. Preliminary crater count ages for the channels and plains are Late Noachian to Late Hesperian with channel and crater fills possibly Amazonian.

Common characteristics. These drainage systems are smaller than the outflow channels but they also have a wide, flat channel or valley. The mapped systems do not exhibit the classical outflow channel morphology such as streamlined islands with crater heads or longitudinal groove systems. Instead, these systems have thick channel fills, that in places appear to bury the channel walls. Narrow inner channels are present within the wider channels along some segments and may indicate that these fluvial systems are ephemeral. In some deposit-dominated reaches, no channel is visible, however, the channel re-appears further downstream. Deposits are identified from streamlined margins, flow-lines, smooth surface, and dark THEMIS Night IR signature. In several places, the wide channels become narrow and deep where they cross degraded crater rims suggesting active downcutting through the rim material. These incised reaches are followed by reaches where where the channel widens and sediments from the crater rim are deposited downslope. Some channels contain possible splay deposits and deltas. Although these might have been easiliy buried with time, we did not identify any evidence for fluvial dune-like features in these channels at CTX resolution and HiRISE images only cover a few channel segments in these areas.

System A: Drainage system A is located on a gently sloping, relatively flat, peak-free, wedge-shaped plain. This is the main drainage for these plains and it contains few tributaries. Near its beginning, the wide channel contains an assemblage of sinuous ridges, cracked mounds and smooth-surfaced channel fill materials. This pattern is repeated downslope. The channel system crosses two degraded impact craters.

System B: Drainage system B is characterized by more deposit-dominated reaches. Although these are probably bedrock channels, the smaller channel seems to be covered by the ejecta of a fresh, 4.5-km-wide crater.



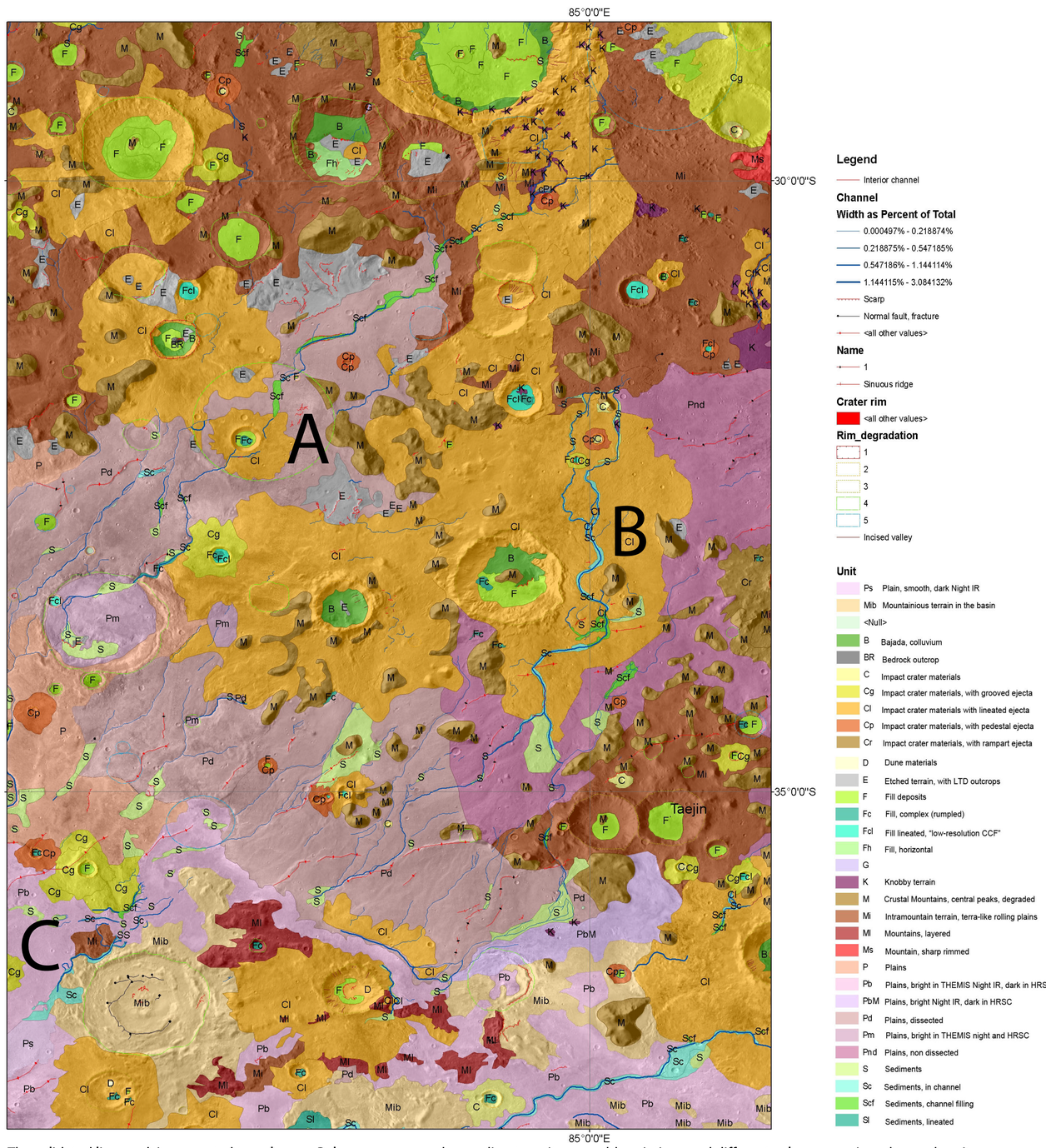
Width and depth of channels >400 m wide in NE Hellas.

System C: This system has two subsystems separated by material that is bright in THEMIS Night IR. Both subsystems begin with several theater-shaped heads, suggesting that they may have formed by sapping.

Implications: NE Hellas basin drainage systems are unlike either the valley networks or the outflow channels. Instead, these systems consist of long channels with alternating reaches, depending on local topography consisting of wide bedrock channels, incised bedrock valleys, and sediment-dominated reaches containing alluvial ramps (gently sloping alluvial cones). Such morphology is consistent with fluvial processes where steeper, narrower segments are characterized by downcutting, channel incisement, and erosion and less confined, shallower segments are characterized by deposition as flow spreads out and deposits its sediment load across the surface. These sediment-dominated reaches separated by fluvial sedimentary bars may be interpreted as having a braided channel morphology. This morphology is distinct from the anastomosing patterns, that characterize the outflow channels that are separated by what are interpreted as remnant islands. We propose that this setting is suggestive of terrestrial discontinuous ephemeral stream channel systems [14-16]. If our interpretation is correct, this region displays nonterminal fluvial sediments in much larger abundance than other systems identified on Mars.

Acknowledgement: This research was supported by a senior research fellowship awarded to H. Hargitai by the NASA Postdoctoral Program at the Ames Research Center. V. Gulick is supported by MRO HiRISE CoI funds.

References: [1] Burr D.M. (2011) Geology 39(7):703–704. [2] Burr, D.M. et al. (2004), Icarus, 171, 68–83. [3] Rice J.W, Baker V.R. (2014) Eighth International Conference on Mars. # 1441.[4] Rice J.W., Baker V.R. (2015), 46th LPSC #2979. [5] Balme M.R. et al. (2011) Geological Society, London, Special Publications 356:203-227.[6] Chapman, M. G., et al. (2003) Journal of Geophysical Research, 108 (E10), 5113, doi:10.1029/2002JE002009. [7] Rodríguez J.A.P., et al. (2014) Icarus 242:202-210. [8] Rice, J.W., (2000) LPSC XXXI. #2067. [9] Tanaka K.L., Chapman M.G. (1990) Journal of Geophysical Research 95(B9):14,315-14,323. [10] Leverington D.W. (2011) Geomorphology 132 (3–4) 51–75. [11] Keszthelyi L. et al. (2014) 45th LPSC #1683. [12] Ghatan G.J. et al. (2005) Earth, Moon, and Planets, DOI 10.1007/s11038-005-9009-y. [13] Makaske B. (2001) Earth-Science Reviews 53 149–196. [14] Bull W.B. (1997) Geomorphology 19:227-276. [15] Field, J. (2001) Geomorphology 37:93-104. [16]



The validated line work is converted to polygons. Polygons are named according to unit name abbreviations and different colors are assigned to each unit name. This completes the geologic (surface cover) map. A, B and C are the three main drainage systems, see text for details.

